Investigation into the high-speed laser welding feasibility of tin-plated steels available for three-piece food packaging can manufacture

Shukla, P

Original citation & hyperlink:
Shukla, P 2014, 'Investigation into the high-speed laser welding feasibility of tin-plated steels available for three-piece food packaging can manufacture' *Proceedings of the Institution of Mechanical Engineers, Part B: Journal of Engineering Manufacture*, vol 228, no. 7, pp. 715 – 729
https://dx.doi.org/10.1177/0954405413498729

DOI 10.1177/0954405413498729
ISSN 0954-4054
ESSN 2041-2975

Publisher: Sage

Investigation into the High Speed Laser Welding feasibility of Tin-Plated Steels to be used for three-piece Food Packaging Can Manufacture

Pratik P. Shukla*

Corresponding Author Details*

Pratik Shukla

Lincoln School of Engineering,

University of Lincoln,

Brayford Pool,

Lincoln, LN6 7TS,

United Kingdom

TEL: +44 7739461805

E-mail: pratik.shukla@talk21.com

Abstract

This investigation was focused on the high speed laser welding (HSLW) of 0.4 mm tin-plated steels used for joining together parts of three-piece Food Cans (FCs). The HSLW quality is generally restricted due to several welding discontinuities that occur with change of traverse speed. A study on the production set-up by a FC manufacturer was first addressed and reasons for introducing HSLW were further discussed. A rotary axis as a welding fixture was designed and made to achieve high surface speeds. Thereafter, an experimental investigation was conducted using a CO_2, neodymium-doped yttrium aluminum garnet (Nd:YAG) laser and hybrid of plasma augmented laser welding (PALW) applied to the typical FC material. Conventional welding defects found during HSLW were observed for all three laser welding techniques. However, humping gradients reduced with PALW and penetration was evident up to welding speeds of 98 m/min. Furthermore, the HSLW defects were discussed and possible solutions to eliminate the humps and further work into the application of the HSLW process for the Canning industry were mentioned.

Keywords: Lasers; Hybrid; PALW; High Speed Welding; Tin-plated steel; Food Cans

1. Introduction

1.1 Background of Food Packaging Can Manufacturing

Increase in population in urban areas and fast-paced lifestyle requiring ease and convenience has slowly given a rise to a variety of new food products which has increased the demand for food packaging containers around the world. In particular, the metallic food cans which are easy to recycle and successfully provide food storage. This surely affects the beverage, drinks and food packaging industry in the United Kingdom (U.K), as 3.8% rise around the world in the demand for food packaging product is expected year-on-year from 2008 through to 2013 [1]. Having said that, the food and drinks manufacturing has only reduced by a small amount throughout the recent recession and the recovery of production output for food and drink products returned rapidly to prior recession times in U.K. [2]. This goes to show that the future for food packaging products such as metallic beverage and food cans is certainly bright.

A rapid increase in the launch of new food products has led a U.K. based food can (FC) manufacturer to produce volumes of 144 million units per annum. On account of this, it can be postulated that the demand for three-piece FCs is not only in the U.K. but in Europe and around the world are also considerably large. In addition, the production speed at which the manufacturers are required to produce each unit is also significantly high since the packaging FC manufacturers are required to produce in masses rather than batches. Moreover, the current technique of joining such three-piece packaging FCs is a mash seam welding (MSW), otherwise known as resistant seam welding technique. This technique has several flaws within the process which are namely: high set-up times, lack of flexibility, technical limitations, wastage of material and lead-times. In particular, the MSW process comprises of a lap joint configuration to form the weld seam. However, lap joints utilize excess material in comparison with butt joints which would waste material every time a three-piece FC is manufactured. The numbers become considerable when adding the annual cost and the amount of the wasted material in dimension. In addition, MSW systems lack the versatility and the flexibility to weld different shapes and sizes of the FCs since the MSW machinery is only set to join one certain can diameter. Hence, upon a change in demand to join another can diameter would require lengthy machine set-ups and timely changeovers during MSW. On account of this, it is required that an alternate process such as High Speed Laser Welding (HSLW) is considered. This research was focused on a case study of a U.K. FC manufacture in relation to the constraints with the current FC manufacturing process and a feasibility study of implementing laser welding as an alternative as well as a superior joining technique.

1.2 Previous Research in High Speed Laser Welding

An increase in the welding speed results in discontinuities within the weld bead. The welding defects are known as humping, undercut and ropy bead [1-4]. Humping is a continuous bulging effect of the weld face in the direction perpendicular to the traverse direction of the laser beam [1-8]. There are three stages in the process where humping is the final stage. As the weld speeds increase, irregular under cutting begins to occur, this leads to the formation of a ropy bead. The second stage will consists of both of the features. However, undercut is formed consistently until the speed begins to increase. Formation of the hump occurs at the highest traverse speed. Humping was first identified by Bradstreet *et al.* [3] in 1968 who followed an investigation into manual metal arc (MMA) welding defects. Gratzke *et al.* [4] presented a theoretical model of the humping phenomenon during conventional HSLW. Main results found from the theoretical work of Gratzke *et al.* was that the quantity of width-to-length ration of the weld-pool remains under critical value for humping to occur. In other words, by maximizing the length-to-width ratio could result to avoiding the hump within a weld-pool.

An investigation by Mombo-Caristan *et al.* [5] used an oblong beam at high speed, bead-on-plate laser welding and reduced the humping effect on 1.3 mm galvanneal sheet steel. Braunsteiner *et al.* [6] investigated the possibility of using a CO_2 laser for HSLW various ST 14 type steel of 1.6mm thickness and showed that a CO_2 laser would be a relevant source to use for this technique. However, no other type of discussion was held with regards to the quality and the associated weld. Cao *et al*. [7] used a 4kW neodymium-doped yttrium aluminum garnet (Nd:YAG) laser to investigate the effect of the welding speed on Ti–6Al–4V alloy sheets of 1 and 2mm thickness. The effects of welding speed on surface morphology and shape, welding defects, microstructure, hardness and tensile properties were investigated. Results were reported to consist of weld joints comprising of only minor cracks, porosity and shape defects were to be seen. Kabir *et. al.* [8] studied, the weldability of 5.1mm thick Ti-6Al-4V sheets by employing continuous wave (CW), 4 kW Nd:YAG laser. Welding speeds were varied and as result. Defects such as under-fill and porosity were observed. Although, welds without cracks were also obtained using a high power Nd:YAG laser.

Blundell *et al*. [9] conducted an investigation on the laser welding of thin sheet steels of 0.16mm to 0.4mm thickness using high welding speeds. Blundell *et. al.* reported the occurrence of discontinuities such as humping and undercut resulting after reaching sufficiently high speeds. Experiments were conducted using a 2 kW Nd:YAG laser alone and then DC plasma augmented laser welding with speed ranging from 10 m/min to 90 m/min. The HSLW discontinuities were minimized with full penetration (of the plastics coated thin sheets of steels) was obtained when the hybrid welding process was employed [9]. It was reported that it is possible to double the welding speeds in comparison with the laser alone welds. The overall hybrid welding results show defect-free welds in comparison with the laser alone welds. However, the work of Blundell *et. al*. still showed presence of undercutting and a raised bead centre. Page *et. al.* [10] later published a study with Blundell to demonstrate successful effects of plasma augmented laser welding not only with high speeds but also with welding tailored blanks as used for the automotive manufacture [10]. Moreover, Russ *et. al.* [11] also investigated the weldability of metal sheets of various thicknesses using a CO_2 and a disc laser. The main results reported evidence of humping, particularly when using a welding speed up to 45 m/min. An investigation by Soderstrom and Mendez [12] reported the theory of humping from undertaking an experimental investigation. Soderstrom and Mendez reported that humping affects result when welding is conducted at high traverse speeds, particularly for thin sheet metals. This focuses on particularly the arc welding process and it does not agree well with the work of other investigators.

1.3 Research Rationale

The study herein first shows an in-depth analysis of the production set-up of one of the leading U.K. based FC manufacturers. This demonstrates the potential cost reduction and savings if HSLW is to be implemented in place of a MSW process. Secondly, this study also demonstrates an experimental investigation of HSLW of tin-plated thin sheet steels used for FCs. Effects of the HSLW process were investigated by a microscopic analysis to observe if the occurrence of the aforementioned welding discontinuities namely: humping, undercut, ropey bead and drop outs after the HSLW process took place. Series of experiments were conducted using a high powered CO_2 and Nd:YAG laser. On this more, a novel rotary fixture was made to obtain high traverse speeds. This was associated by a robotic motion system and also by applying an additional heat source of the plasma augmented torch. Owing to this, it was then not only possible to achieve high welding speeds but also to understand as a first-step, the effects of HSLW thereon the FC material.

2. Analysis of the FC Production Set-up

2.1 Production system for three-piece FC Manufacture

From analyzing the production set-up of a leading beverage and FC manufacturer in the U.K., it was found that requirements are such that the production rate was 500 cans/min. The company uses 10 hours per shift on a 2 shifts per day regime. This meant that 600,000 units of the three-piece FCs are produced per day. After calculating the quantity per week considering 48 weeks of operation per year, the production of the three-piece FCs was 144 million annually. The calculated values are further presented in Table 1.

Table 1 A summary of a can manufacturing production rate.

Manufacturing/Production Rate	Quantity
Number of hours per day	10
Shifts per day	2
Production rate (units/min)	500
Units per day	600,000
Units per week	300,0000
Units per year (48 weeks/year)	144 million

The FCs come in two forms – either two-pieces or three-piece which differentiates them from the two-piece aerosol cans and the required process to join each can. Most of the cans are made from a two-piece body with the top part of the can as the second piece being made from the same material. The two-piece cans are made using press working and deep drawing process where the sheet metal is blanked into large disks and pressed into cup shape that is further deep drawn to form the body and base of the can [13]. The drink is then filled and the top is joined by a flange joint. However, manufacturing of a three-piece FC is somewhat involved and comprises of several steps further described elsewhere [14].

2.2 Mash Seam Welding and High Speed Laser Welding Process Steps

The FC comprises several steps for its manufacture from raw materials to a finished product as presented in Figure 1(a). First, a large coil of 0.4 mm thick steel is cut into small sheets. Then a layer of tin is applied to the surface of the sheet steel which becomes the internal surface of the FC. The special tin coating provides a protection from any interaction of the metal to the content inside and possibility of corrosion. The tin-plated sheets are then cured in an oven at high temperature. The large sheets are then slit into smaller sheets to the exact dimensional size to form the body of each can. Each sheet is then rolled into a cylinder by rollers installed into the mash seam welding machinery. The edges of the cylinder are welded by the MSW process. The material at the intersection of the welding point is free from the tin coating which enables a sufficient joint to be produced. The welded surface (weld bead) inside the can is yet vulnerable to contamination and corrosion so it is then treated with the tin coating, continuously running over the seam line of the weld. The tin-plated surface is cured by blowing heated air on the outside of the can body. The cans are then passed through a flanger to allow the end of the can to be flanged (except the top and the bottom part). This is a specialized flanging machine which carries out this process. Blank ends are also prepared by the aid of press work to form the disc shape. This is the second piece of the can which is attached to the flanged end of the can body by the aid of a flange joint technology. The cans are passed through a beader to give an added strength to the structure, the beader forms a wrinkle structure on the can body which adds rigidity and takes in account for the volume changes. Cans are then passed through a pressure tester for any impurities, pinholes or larger fractures which may have occurred on the surface. Defective cans are automatically rejected. The finished cans are then palletized for dispatch to the filling plant. The third piece of the can is joined after the can has been through the filling process which is also carried out at the filling plant.

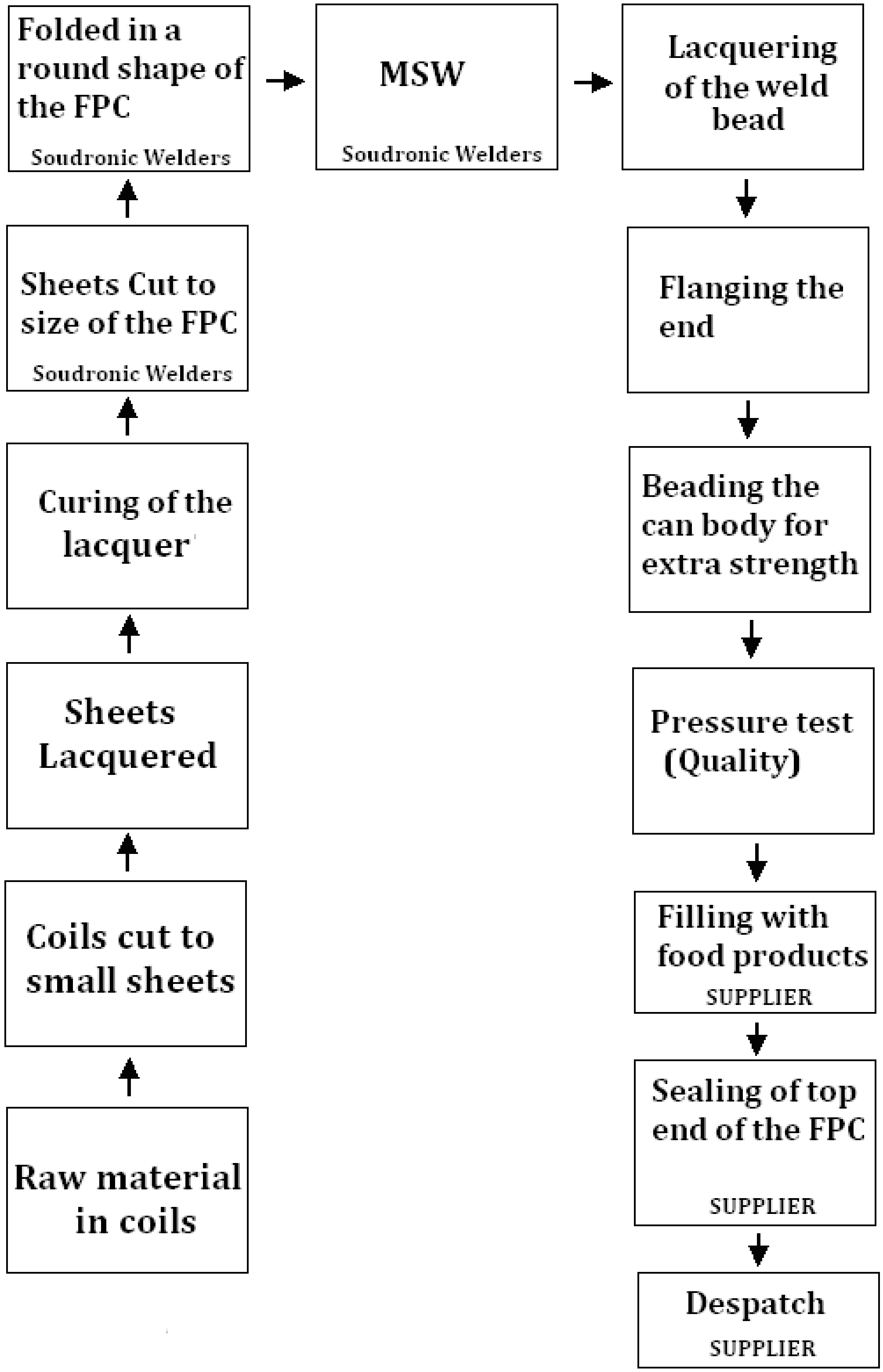
Folded in a round shape of the FPC
Soudronic Welders
MSW
Soudronic Welders
Lacquering of the weld bead
Sheets Cut to size of the FPC
Soudronic Welders
Flanging the end
Curing of the lacquer
Beading the can body for extra strength
Sheets Lacquered
Pressure test (Quality)
Coils cut to small sheets
Filling with food products
SUPPLIER
Raw material in coils
Sealing of top end of the FPC
SUPPLIER
Despatch
SUPPLIER

(a)

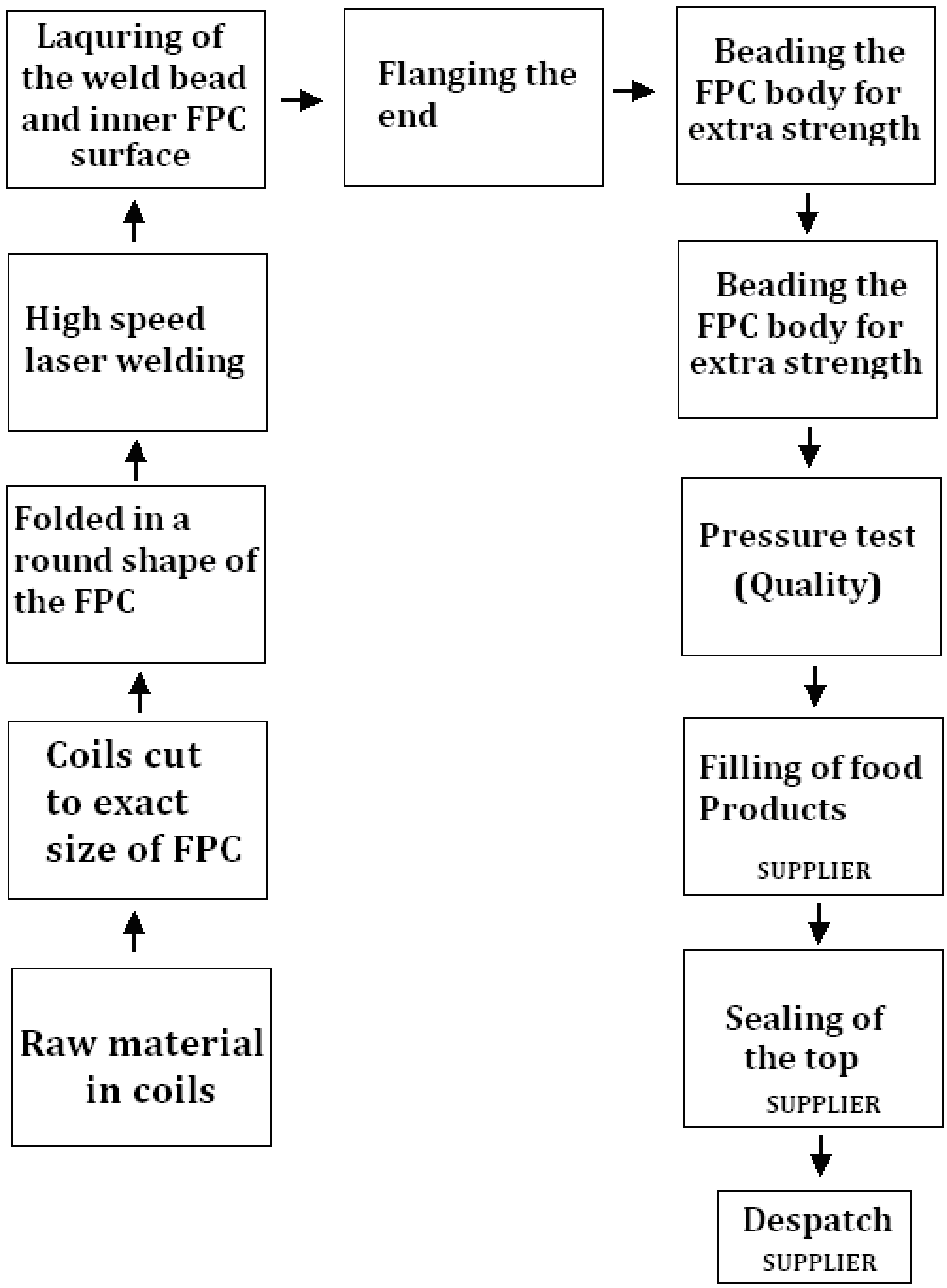

(b)

Figure 1 A Schematic diagram of the MSW process in (a), and (b) the HSLW process.

As seen from Figure 1(b) that the process steps needed for the HSLW are reduced in comparison to the MSW. This is because the tin coating process is not required to be completed twice prior to the mash seam welding and after, for coating the weld bead in the case of the current MSW process (see Figure 1(a)). In comparison, the HSLW process could include the tin-plating step after the laser welding process has taken place. This would eliminate the lead-time to make the FC and increase the throughput within the production line.

2.3 Rationale for implementing High Speed Laser Welding

Overlapping joints have tight tolerances. The diameter of a three-piece FC is usually 78mm, 96mm, or 110mm. FCs come in various lengths: 50 mm, 90 mm and 110mm. The MSWed bead of a three-piece FC is 1.5mm as shown in Figure 2. The MSW technique produces a lap joint by over-lapping the two opposite ends of the FC. A cross-section of a MSW lap-joint is shown in the microscopic image in Figure 2 of a tin-plated three-piece FC. In comparison with a butt joint, the lap joint utilises excess material which means that there is a small amount of material waste with every single three-piece FC that is made. When the material waste is calculated annually, then the numbers become significantly large. The HSLW process on the other hand has the potential to weld with a butt joint configuration. This means that there will be a considerable saving in the use of material to form the three-piece FC body. The savings in the material usage, in turn, could result in extra production capacity or simply a reduction in lead-time. This consequently, could result in considerable cost reduction by reduced labour, operational hours as well as reduced electricity costs and overhead.

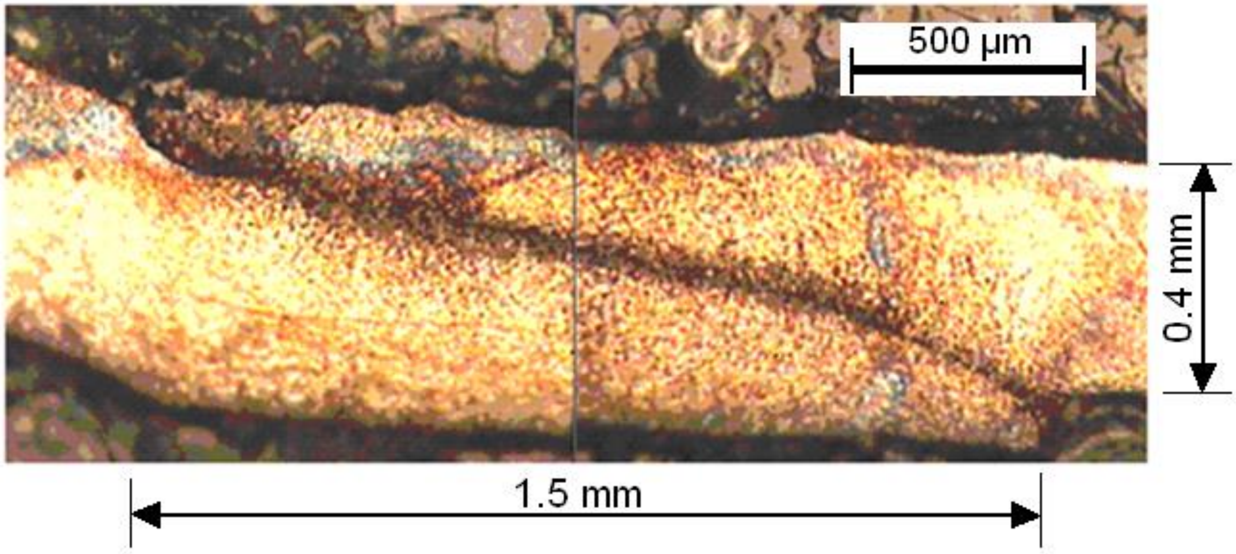

Figure 2 Optical image of the cross-section of a MSWed joint, showing the thickness of the FC wall made from tin-plated sheet steel and the amount of over lap used.

In addition, the MSW machinery is not flexible enough to weld different shapes and sizes of the FCs. Each MSW machine is set to a limit for joining a certain diameter of the three-piece FC. For example can diameters of 78mm, 96mm and 110mm for welding are generally set within the RSW machinery. When the demand changes for joining a different diameter, then the MSW system cannot easily accommodate the change since time consuming set-ups are required. The smallest weldable can diameter is 38mm due to the smallest sized rollers available within the MSWer which prevents MSW of small diameter cans such as two-piece aerosol cans and therefore, are naturally forced to be joined by using alternative techniques. In comparison, the HSLW system could accommodate the joining of a variety of can diameters since there are no restrictions on the use of rollers. Thus, it is feasible to join small to large can diameters of varying lengths including not only the two-piece aerosol cans but larger cans used for storage of liquid food, animal food and other products such as containers for paint, oil, and chemical storage.

The daily machine warm-up time of the MSW machines is around 15 min. However, it could take up to 8 hours to set-up the machine if there is a requirement to change can diameter since a considerable amount of machine set-up is generally required. Consequently, 5 skilled operators are required to complete the task. In addition, the machine undergoes a maintenance procedure every six weeks. Most working parts are serviced and small size parts are replaced if wear and tear is present. This adds an additional maintenance cost. In comparison, a HSLW process requires a minimal daily maintenance to start-up the laser system. Hence, the set-up times are in minutes rather than hours if appropriate jigs and fixtures are employed and a sufficiently skilled, single operator is also capable of setting-up the new product/part on the laser system. Moreover, the new laser systems are now almost maintenance free and require very little attention on a regular basis. So the frequent maintenance is no longer required and rather than weeks, the maintenance procedure is conducted every 4 to 6 months for the HSLW process.

The MSW system contains 60mm diameter rollers rotating at 500 rpm, achieving speed of 47.12 m/min at the welding interface. A laser system, in comparison, using a correct set-up is capable of achieving much superior speeds of 130m/min with great accuracy and tight tolerances [15, 16]. Furthermore, some welding impurities such as formation of nuggets on the weld seam tend to occur with the MSW process which means that the FCs must be scraped eventually and sent for recycling. However, the feasibility of HSLW as yet is a question which needs to be answered? This will be the next-step of the investigation which will be presented with the aid of the experimental investigation as presented further in this paper

2.4 Cost Reduction and Savings upon Implementing High Speed Laser Welding

Tight fit-up joints and good tolerances are achieved by the use of laser technology [10, 17 - 18]. As mentioned before the, utilisation of a butt joint configuration could minimise the amount of material required to join the FCs. If a butt joint configuration using HSLW is employed then the amount of excess material saved can be calculated annually from the optical image (see Footnote 1). Considering a 96mm diameter FC as an example would result to material savings/can as presented in Footnote 1, followed by the wastage of the total can production in a year for that particular can diameter, if the butt weld configuration is adopted using HSLW in place of the conventional lap welding method using MSW. Figure 3(a) illustrates a schematic of the flat sheet main body of the FC showing various dimensions. Figure 3(b) illustrates a schematic of the RSWed with dimensions and Figure 3(c) is an optical image of the RSWed main body of the tin-plated FC.

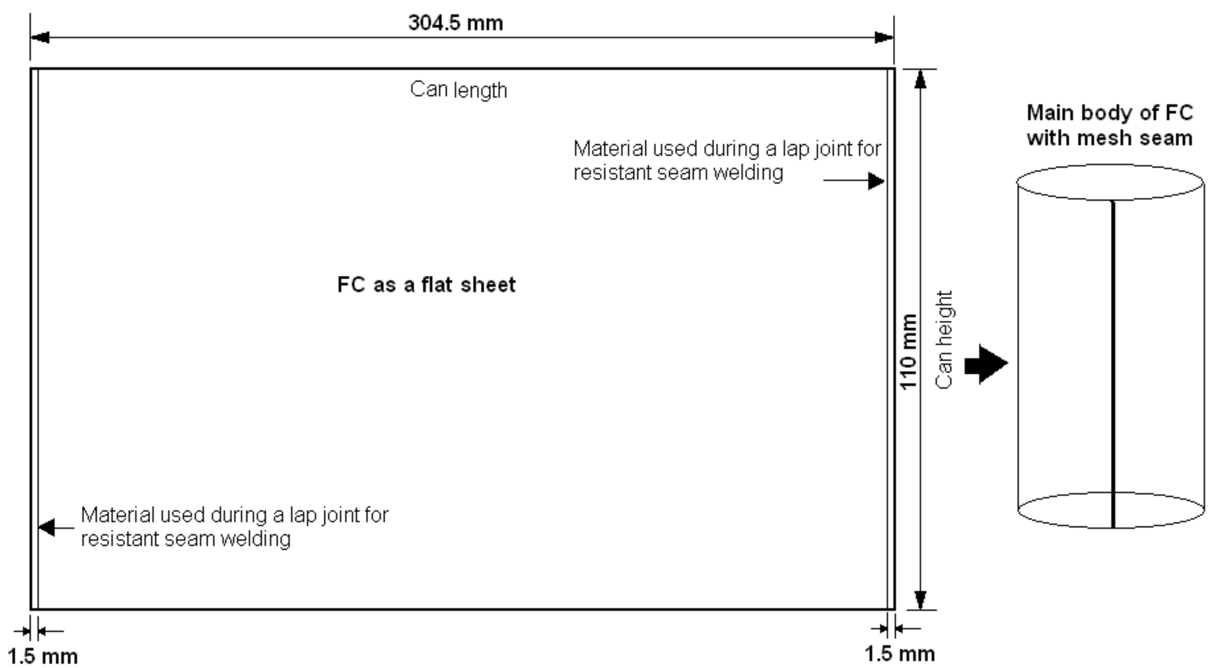

(a)

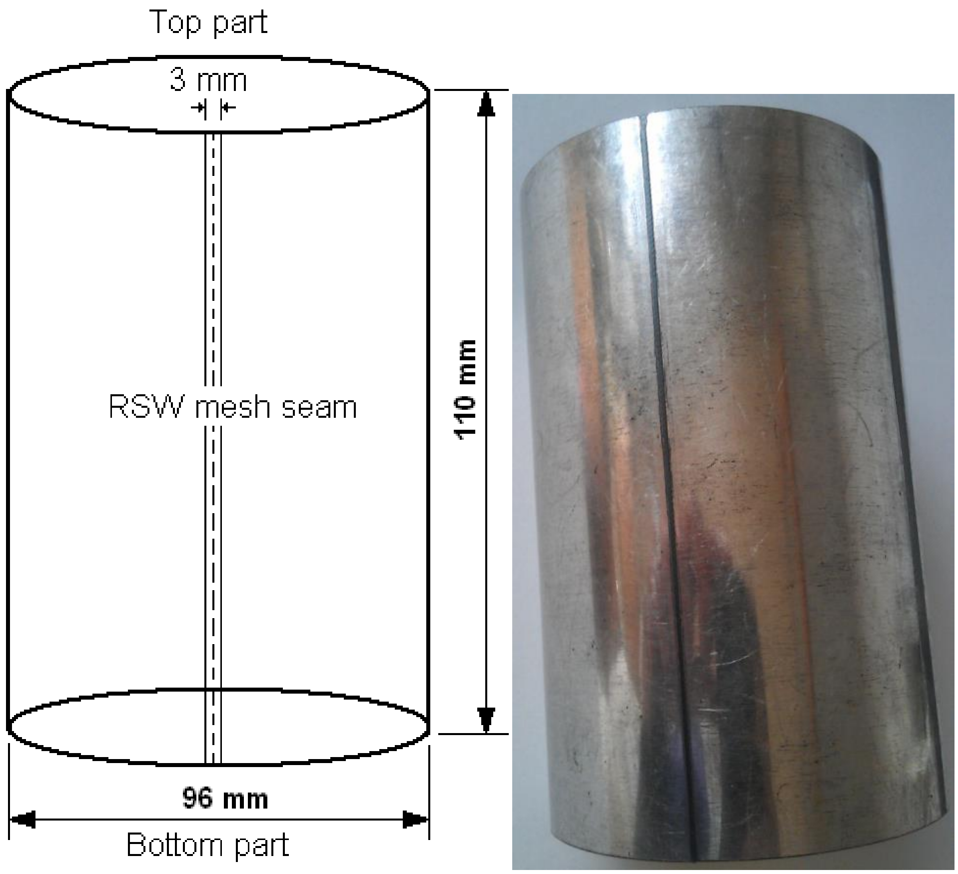

(b) **(c)**

Figure 3 A schematic of the flat sheet main body of the FC in (a), a schematics of the RSWed FC in (b) and a image of the RSWed main body of the tin-plated FC in (c).

This means that by saving material it is possible to either increase production output or cut down the number of hours required to reach the current production volume, since it will be possible to manufacture more units in the same time period when implementing the HSLW technology. Therefore, either the production volume can be increased in the same amount of lead-time or alternatively, the lead-time can be reduced to produce the equivalent number of units as required for the current demand. The reduction in materials waste in turn would leads to commercial advantages to be gained by the aforementioned FC manufacturer as can be seen in Footnote 1

FOR EDITORS: PLEASE PLACE THIS TABLE AS A FOOTNOTE IF POSSIBLE.

Footnote 1

Analysis of Production System	Units
Can diameter, Can Height Can Length, Area	96 mm 110 mm, 304.5 mm, 33495 mm^2
Cost of manufacturing one FC (unit)	£ 0.12
Material wastage per FC (unit)	1.5 mm x 110 mm = **165 mm**
Material saved per FC (unit) (see Figure 3)	165 x 2 = **330 mm^2**
Material saved/year	330 mm^2 x 144 000000 (Units) = **47520000000 mm^2**
Required material to form the first piece of a can (96 mm diameter, 110 mm length)	**33495 mm^2**
Material wastage per can (96 mm diameter and 110 mm length)	**330 mm^2**
Material waste per year	**47520000000 mm^2**
Extra production subject to material saved for 96mm diameter of FC	47520000000 mm^2/33495 mm^2 = **1418719 units/year**
Potential savings from material reduction for one type of three-piece FC diameter	1418719 units x 0.012 (£) = **£17024 .63**
Lead-time savings per/year (for 96mm type of FC)	1418719 units/ 500 (units/min) = **2837.43 min or (47.29 hrs)**
Potential savings from having extra lead-time in production capacity (for 96mm type of FC)	2837.43 min x 500 units = **1418715 units** = 1418715 x 0.012 = **£ 17024.58**

Note: *The above figures are a summary of the potential savings achievable from reducing the material usage and lead-time and are subject to change depending on the demand, and the required production volume at any particular time.*

The savings presented in the Footnote appear to be considerably small, however, it should be noted that the potential saving are as result of one type of can size which in this case is a 96mm diameter can. When other can sizes are taken into account then the savings and the accounted benefits will sum-up to a large number. In addition, it is not simple to account for the amount of units which the HSLW process could produce at this stage in the research but it is worth a mention since a major advantage would result from the fact that a laser system could potentially weld at speeds two folds higher that the MSW technique which is welding at a maximum speed of 47.12 m/min with 500 cans/min. This indicates that an increased productivity, considerable reduction in lead-times and an increased throughput as well as low operational costs, reduced labour and lower maintenance costs could be gained. On account of this, despite the high investment cost of a laser system, the implementation of HSLW could still aid gain and eventually become a profitable venture in a short term rather than a long term. This inherently could prove to be an investment for a fruitful future by not only increasing the output and production capacity, reduced lead-times, considerable material savings but also enabling FC manufactures to gain a competitive advantage and meet the rising demands.

3.0 Experimentation and Analysis

3.1 Experimental Material

The material under investigation was 0.4 mm thick tin-plated steel comprised of electrolytic chromium/oxide coating as used for the FCs supplied by a U.K, based food and aerosol can manufacturer. The tin-plate steel is coated on both sides with pure tin at coating weight ranging from 1 to 12 g/m^2. Flats sheets of size 110 mm (height) x 304 mm (length) were used to conduct bead-on-plate experiments (see Figure 4). The flat sheets of tin-plated test samples were fixed firmly onto the rotary welding fixture as shown in Figure 4(b) which also limited distortion during HSLW.

3.2 Sample Preparation

The laser welded tin-plated steel was later cut through the cross-section of the weld for microscopic analysis. Thereafter, the samples were set into 60% Methylmetacrylate (polymer powder) mixture with liquid 40% Tetrahydrofumfury – Metacrylate (liquid hardener) and were left over night to harden. The samples were then ground and finely polished in stages using 6μm, 3μm and 1μm polishing wheels for 5 min each. Care was taken during grinding and polishing to avoid excess heat transfer to the plastic moulds which otherwise would affect the characteristics of the laser welded region. Thereafter, the samples were etched using 2 to 5% Nital for 30 sec so the cross-section of the welds could be viewed under the optical microscope (Mitotoyo; LWD; Japan).

3.3 Nd:YAG Laser Welding Technique

A 2 kW, CW, Nd:YAG laser fed *via* a 600μm diameter optical fibre to conduct trial on a bead-on-plate experiments. The laser emitted a wavelength of 1.064μm and consisted of a TEM_{01} beam mode with a beam quality factor - M^2 to be 1.3. Argon assist gas was employed at 20 l/min with a spot size of 1mm with an applied laser power of 0.5 to 2 kW. In addition, traverse speed was obtained using a rotary axis fixture between 25 to 100 mm/min. The Nd:YAG laser was assisted by a KC 25, Kuka, 6-axis industrial robot. The Kuka robot was programmed to traverse horizontally in the X direction at low speed in order to create spiral weld lines on the material surface (see Figure 4) as the rotary fixture was made to rotate at 300rpm. The work-piece was held firm using small clamps which avoided distortion to take place. The rotational traverse speeds are measured by a revolution gauge (taco meter) to initially set-up the experiments. The use of the rotary fixture was employed since high speeds can be achieved. More importantly, the robotic motion system comprised of a low dynamic response which meant that for the robot to traverse at a high welding speed required large area. This would allow the robot to ramps up to a maximum set speed from its initial position to weld the work-piece and maintain the speed over the sample, then reduce whilst it is on the path to the initial home position. However, this was not possible to program as it required large traverse area which was not available within the experimental set-up. On account of this, a particularly designed rotary fixture was made and upon a correct set-up enabled to obtain high surface speed processing during the laser welding experiments.

(a)

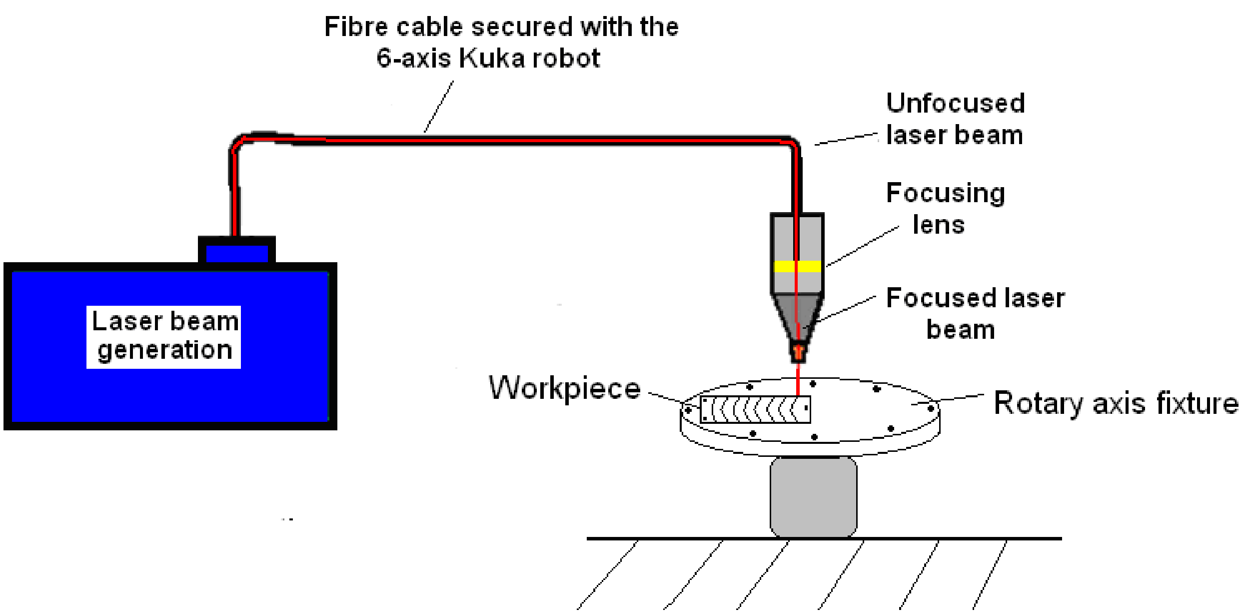

(b)

Figure 4 Image of the Nd:YAG laser assisted plasma torch in (a) and (b) a schematic diagram of the Nd:YAG laser alone experimental set-up with the rotary axis fixture.

3.4 Plasma Augmented Laser Welding (PALW)

The second set of trials used a Nd:YAG laser and a plasma torch as an additional heat source as shown in Figure 4(b) and Figure 5. The rotary welding fixture shown in Figure 5 was designed and made to achieve surface speeds of up to 150 mm/min. This was so because it would suit the nature of the experiments and would allow flexibility to be employed under both types of lasers used for this research. The PALW experiments were conducted using triangulated configuration where the electrical current of 40V flowed through to complete a circuit. The PALW experiments were conducted in similar fashion to previous laser alone experiments but in this case a DC plasma arc torch was attached to the Nd:YAG laser head at 45°. This was because the 45° allowed sufficient coupling of the laser beam and the plasma. In addition, previous experiments also employed similar settings [9, 10]. Spot size of 1 mm, was used with an argon assist gas of 20 l/min. The power was varied from 0.5 to 2 KW using CW mode and the traverse speed was varied in the range of 5 m/min to 100 m/min. Moreover, the Nd:YAG laser comprised of the same features as to the experiments conducted using laser alone trials.

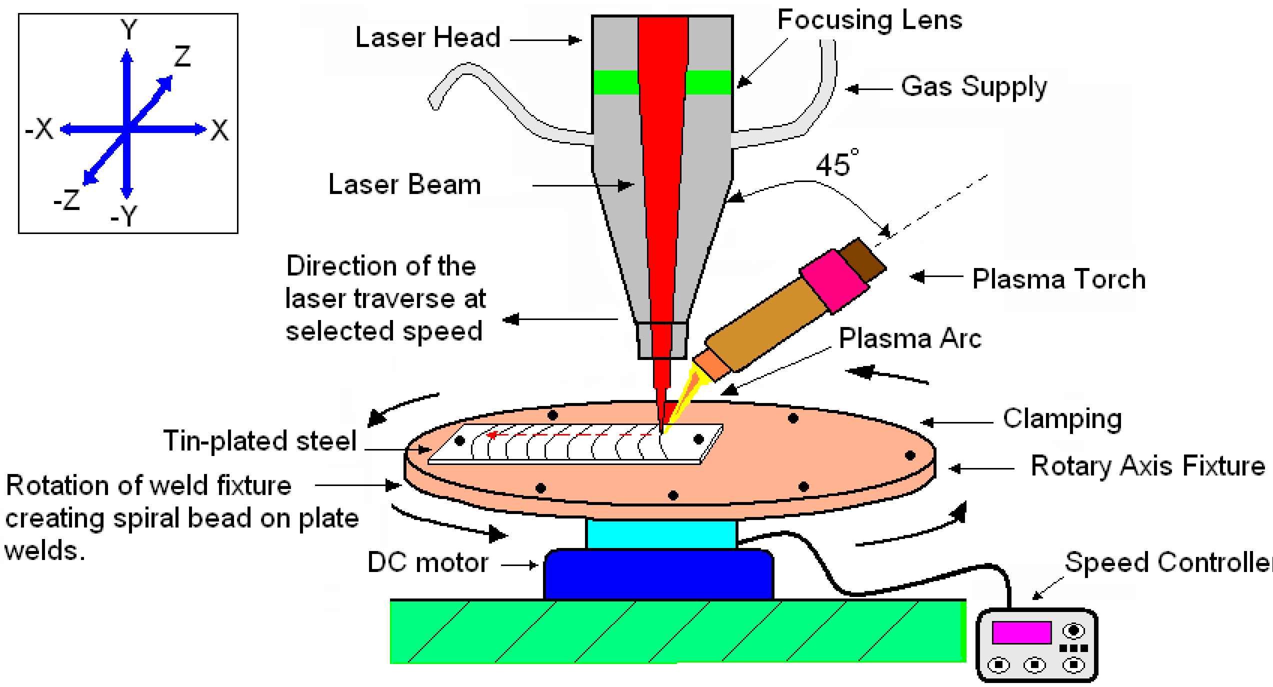

Figure 5 A schematic diagram of the Nd: YAG laser and PALW set-up with a rotary welding fixture.

3.5 CO_2 Laser Welding

A 2 kW CW CO_2 laser was employed to conduct the first-set of experiment. The CO_2 laser emitted a 10.6μm wavelength and had a beam mode of TEM_{00} with an M^2 beam quality factor of 1.2. Trials were conducted between 5 and 100 m/min. High traverse speed was achieved using rotational speed of the welding fixture with the laser power being varied from 0.5 to 2 kW. Argon was used as an assist gas at a flow rate of 20 l/min. The CO_2 laser was programmed to run in a straight line (X direction) at a low speed in the centre of the tin-plated sheet of steel as the rotary fixture was rotating at 300 rmp. This combination produced a spiral welded pattern. The laser beam was switched on and switched off at selected positions on the sample (see Figure 6).

(a)

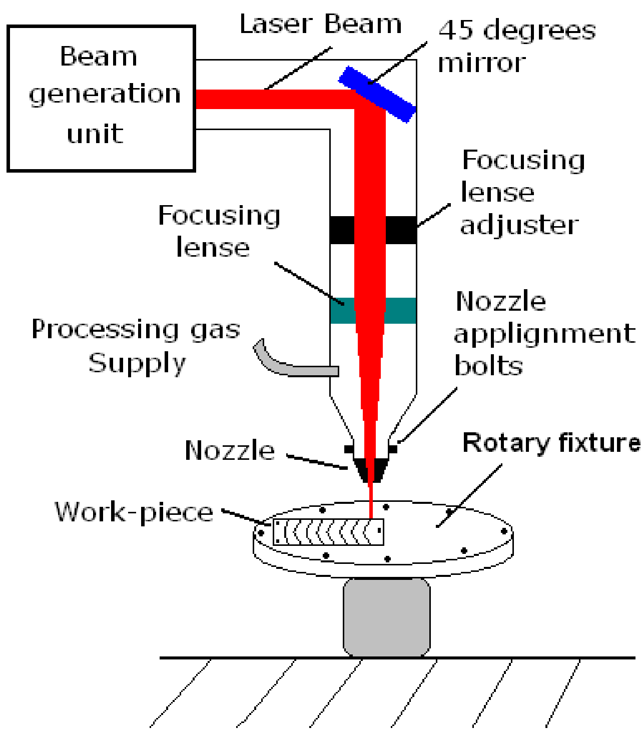

(b)

Figure 6 An image of the CO_2 laser set-up in (a) and (b) a schematic of the CO_2 laser beam delivery system and the rotary axis during HSLW.

3.6 Tensile Testing

The MSW, PALW and both the CO_2 and Nd:YAG laser welded samples of the tin-plated steel was tested for the ultimate tensile strength of the weld seam. Five strips were cut to 10 mm x 50 mm rectangular shape for each of the welding processes and comprised of the weld seam being precisely in the centre of the sample with equal amount of material left on each side. An average was taken for each of the five samples and is further presented in this paper. The samples were placed (one at a time) vertically in the Y-axis into the tensometer (LR50 K plus universal testing machine; Lloyds Instruments Ltd; USA) and pulled apart in a vertical orientation by the tensometer in ambient temperature. The load was consequently increased from 0 N until the sample was completely fractured to obtain a load *vs* extension graph (see Figure 12). The results were naturally generated by the operating software (NEXYGEN*Plus*) of the tensometer and were tabulated in graphical format to show a comparison welded samples.

3.7 Welding Speed Configuration

Due to mechanical constraints, the laser systems employed herein were unable to obtain the desired welding speeds. It was therefore required that the work-piece being welded would traverse using rotational speed to obtain higher traverse speeds during the laser welding process. Therefore, a rotary fixture was designed to achieve surface speeds from 10 m/min to 150 mm/min (see Table 2 and Figure 7 (a) and (b)). This solved the problem of having insufficient dynamic response which the two motion systems had for both the CO_2 and the Nd:YAG laser. On account of this, the speed was first configured by Equation (1):

$$\mathbf{V = \pi \times D \times N} \qquad (1)$$

Where **V** is the velocity, π is 3.141, **D** is the weld diameter and **N** is the number of rotations of rotary welding fixture. The applied welding speeds ranged from 5 to 120 m/min.

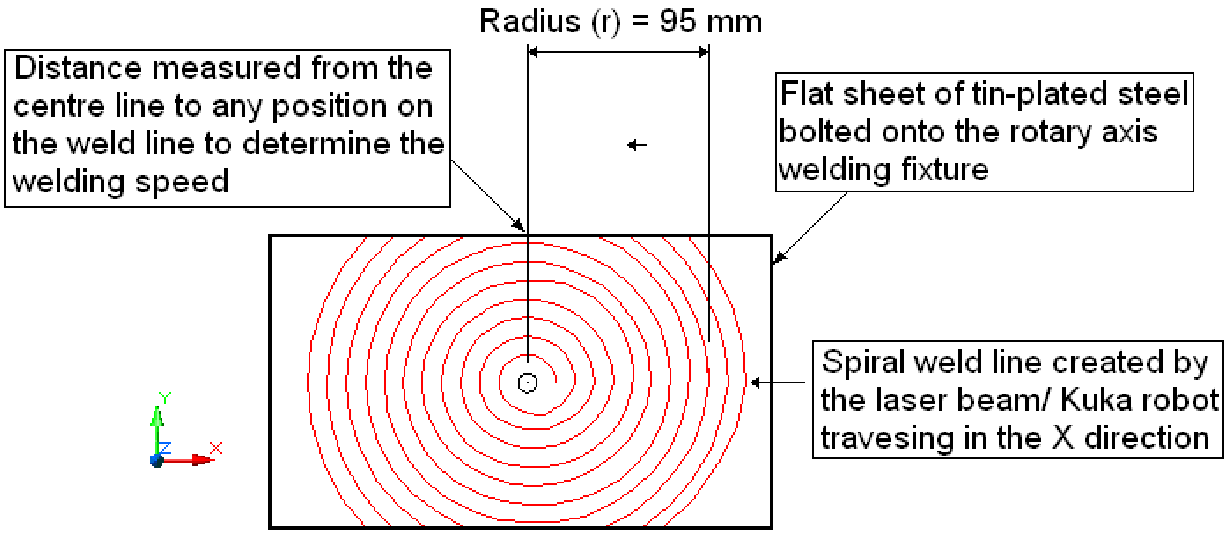

(a)

(b)

Figure 7 A schematic of the traverse speed configuration during HSLW in (a) and (b) an image of the rotary fixture designed for the HSLW experiments.

Table 2 Surface speeds configured at various distances on the rotary fixture according to Equation (1) during all three laser welding techniques.

Selected Distance from the Centre of the work-piece ((r) mm)	Configured Speed (m/min)
5	4.71
20	18.84
35	32.97
50	47.10
65	61.23
70	65.94
85	80.07
110	103.62
125	117.75
140	131.88
155	146.01

4. Results

Figure 8(a) to (e) illustrates the Nd:YAG laser welded images of the tin-plated thin sheet steels at varying speeds. As shown in Figure 8(a) to (e), humping phenomenon exists to some extent. In Figure 8(a), the optical image represents the cross-section of the sample welded at 10 m/min. The depth of penetration at this position as shown in Figure 10 is about 50%. Then as the speed increases, the depth of penetration reduces due to the lack of thermal energy induced into the material. Using the Nd:YAG laser alone technique, beyond 70 m/min, humping was not found and only a small heat affected (HAZ) was to be seen with penetration of about 5 %. It is obvious that this affect would occur since the increase in the traverse speed would result to a decrease in the thermal energy induced into the material which thereby reduces the laser-material interaction time and consequently reduces the depth of penetration. The results of the Nd:YAG laser alone weld samples complied to the results of a few previous researchers that stated that humping resulted at lower speeds during welding of the thin sheet steels and with increasing speed, the gradient of the humps reduced.

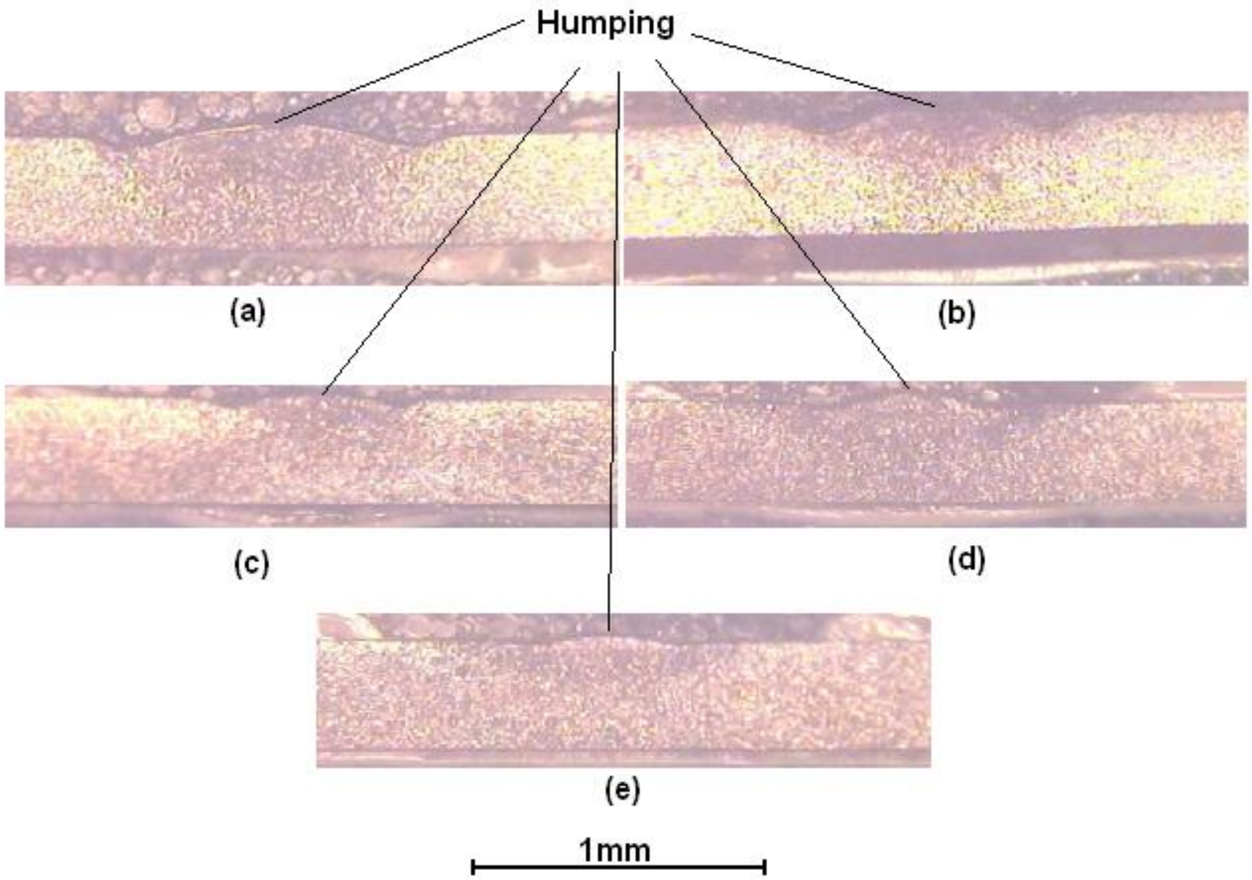

Figure 8 Optical image of the Nd:YAG laser alone welded sample in (a) at 10 m/min; (b) at 30 m/min; (c) at 50 m/min; (d) at 60 m/min; (e) at 70 m/min using a spot size of 1mm; laser power of 2 kW; argon assist gas with a flow rate of 20 l/min.

The results in Figure 9 revealed that by applying the PALW technique, the humping effect was much reduced due to the extra heat source. The use of plasma torch enabled an increase in temperature at the laser-material interaction zone and allowed larger melt zone to occur in comparison to the laser alone welded samples. The melt zones upon freezing resulted to a smaller gradient. Although, penetration reduced with increase in the weld speed, there was still some effect of the PALW up to 98 m/min. This in comparison to the finding by Blundell *et al.* using the PALW welding process was similar [9]. However, it was possible to obtain higher speed using the set-up of the study herein since a rotary axis welding fixture was employed. On the other hand, due to the lack of dynamic response of the motion system employed in the work of Blundell *et.al.,* the maximum weld speed achieved with only a few welding discontinuities was 90 m/min.

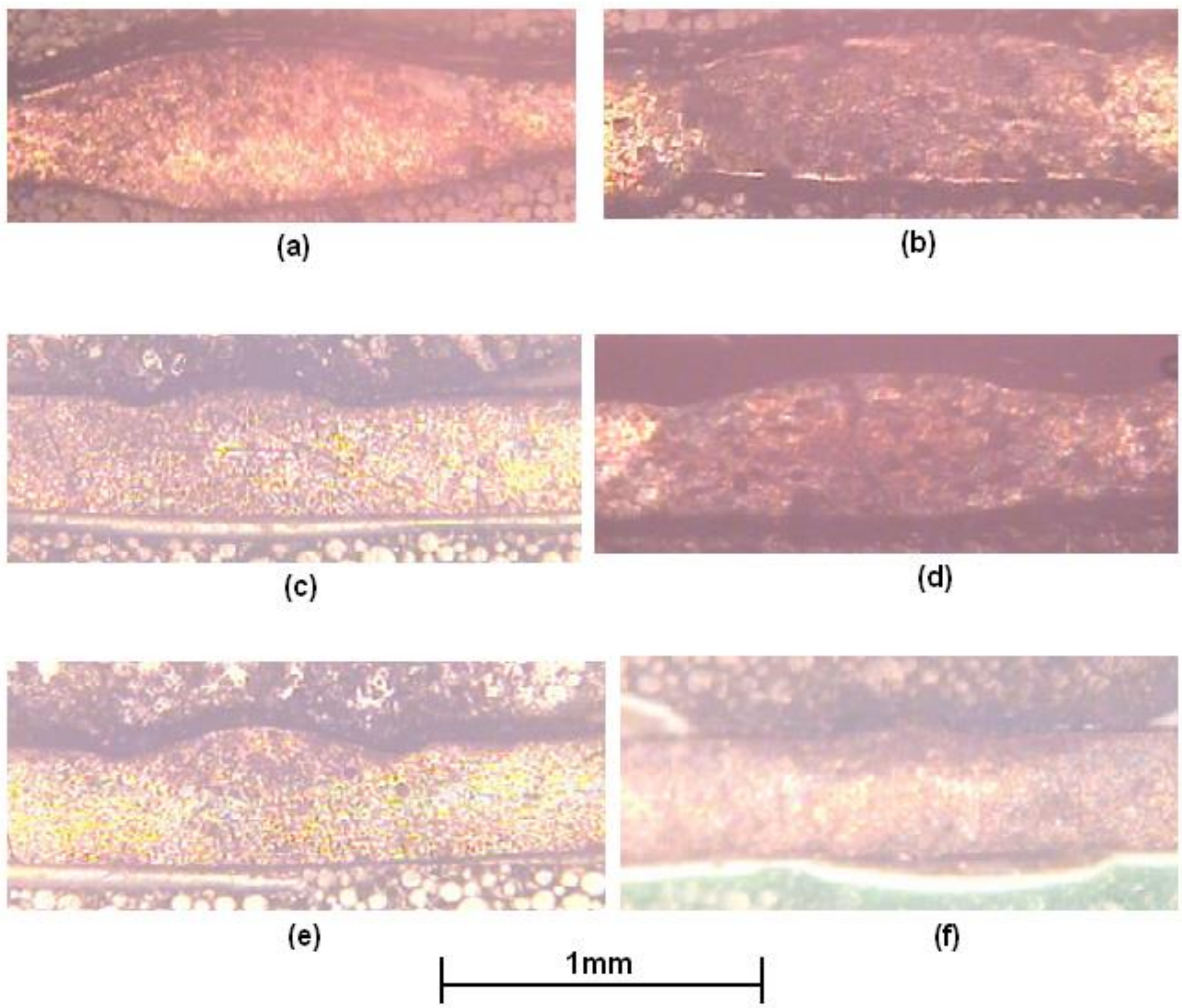

Figure 9 Optical images of the PALW using the Nd:YAG laser in (a) at 10m /min; (b) at 40m/min; (c) at 77 m/min; (d) at 30 m/min; (e) at 65.94 m/min; (f) at 98.43 m/min using 2 kW laser power; 1 mm spot size; a voltage supply of 40 v through the plasma torch and argon assist gas with a flow rate of 20 litre/min.

Figure 10 shows a speed vs penetration graph for the three welding processes used in this study. The curves in Figure 10 shows that the penetration of the PALW samples is much greater followed by the CO_2 and then the Nd:YAG laser welding technique. However, due to the laser beam quality factor M^2 of the CO_2 laser being a high quality beam resulted to a much concentrated beam that exhibited large impact which in turn during surface speed of 33 m/min and below produced considerable drop-outs where the beam had created a hole into the tin-plated thin sheet steel. This effect was also seen with the other two welding techniques, however, to a much smaller extent at low speeds. As the traverse speeds increased, a reduction occurred not only in the penetration but also with the humping phenomenon.

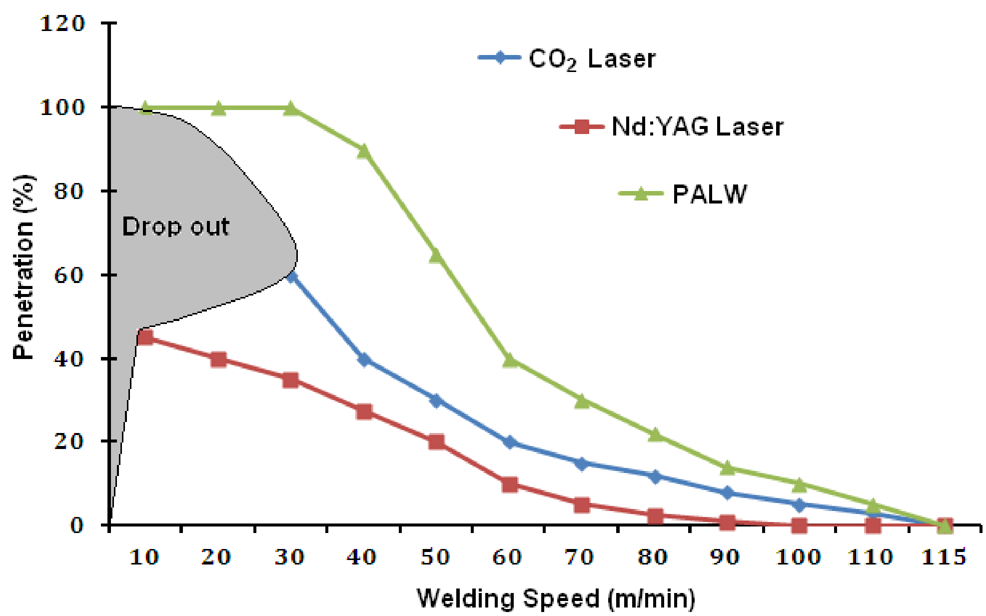

Figure 10 The curve shows the weld penetration with increasing speed when using the CO_2 and Nd:YAG laser alone and PALW.

Figure 11 shows the results of the CO_2 laser welded samples of the tin-plated thin sheets steels. In comparison to the results obtained by the Nd:YAG laser alone and to those of the

PALW samples, it was found that the gradient of the humps observed were much steeper at lower speed and then became smaller. In any case, the humping gradient was yet much greater than with the previous two (Nd:YAG laser alone and PALW) techniques. At the same time, the penetration of the CO_2 laser beam began to deteriorate. This could be attributed to the absorption of the tin-plated steel being somewhat lower than that of the Nd:YAG laser and the PALW. Nevertheless, the absorption of different wavelengths by the tin-plated thin sheet steel is yet to be confirmed by an experimental study in future investigations. What is more, the causes for the humping effect could be wavelength dependant since the Nd:YAG laser produced smaller humps than the CO_2 laser. Having said this, further study is also required using more than just two wavelengths to conclude as to what extent the wavelength contributes to affect the humping phenomenon. It can be gathered that the characteristics of the laser beams used has first caused this effect to take place, whereby the CO_2 laser exhibiting a much higher beam quality would have induced higher thermal energy focused in a localized surface area. This caused an instant bulging of the melted material and created significantly large peaks in form of humps whilst the Nd:YAG laser comprised of a top-hat beam. This distributed over a larger surface area and relaxed the hump to take place. Moreover, the PALW technique not only exhibited a broader beam but also applied an extra heat source which trailed after the Nd:YAG laser, elongated the cooling rate and allowed the weld-pool to solidify at a considerably slower rate than the CO_2 and the Nd:YAG laser alone weld pool. This maximized the possibility of distributing the melt-pool evenly and produced a much relaxed humping gradient as well as penetrating much further into the material unlike the Nd:YAG and CO_2 laser alone welding techniques.

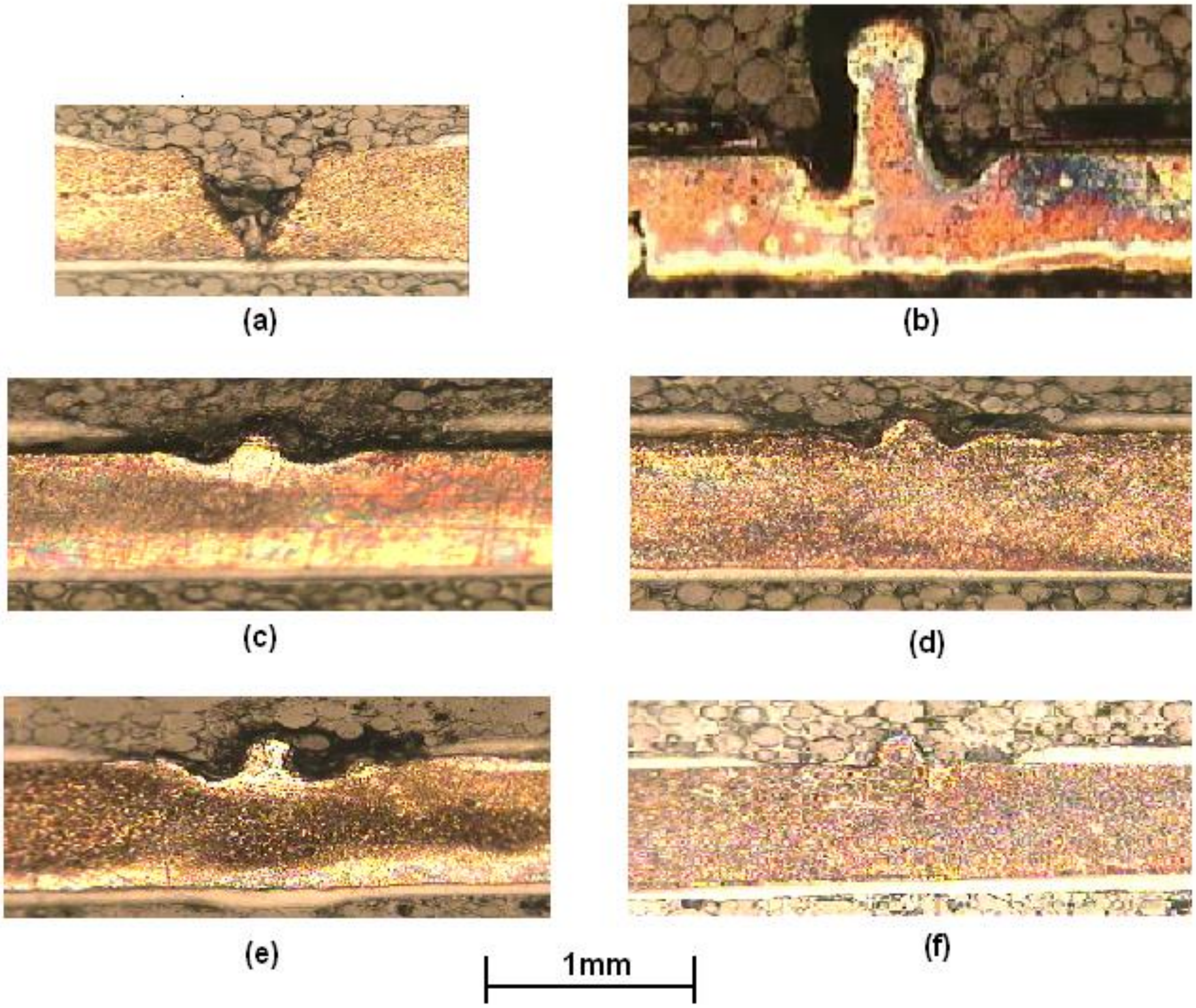

Figure 11 Optical image of the CO_2 laser welded samples in (a) at 20 m/min; (b) at 42 m/min; (c) at 60.52 m/min; (d) at 80 m/min; (e) at 90 m/min and (f) at 105 m/min by applying 2 kW laser power; spot size of 1 mm; argon assist gas at a flow rate of 20 l/min.

Having observed the results obtained from the experiments in this study, it is an interest to first understand the laser-material interaction in order to know how? and why? the humping effect was caused so that it can be either avoided or eliminated in future investigations. From the optical images in Figure 8, Figure 9 and Figure 11, it can be seen that humping is considerably high during lower traverse speed welding and with increase in welding speed; the gradient of the humps began to slack. This change in the weld profile resulted from the actual melt-pool starting-off as a keyhole weld where the energy of the laser has time to absorb into the material surface and penetrate through the sub-surface and the cross-section whilst the speed increases, the keyhole of the weld becomes smaller as conduction welding begins to take effect with the laser beam not having enough time to absorb into the material. This allowed the humping effect to relax with increasing speed.

Furthermore, humping is also caused by a pinch effect on the longitudinal direction of the weld bead. The surface tension caused within the weld bead is due to the Marangoni convection where instability in pressure causes the regime of high and low curvature which in turn could also lead to the humps.

During cooling of the weld, rapid solidification takes place since the high power density of the laser was focused on a small surface area not allowing enough time for the surface and sub-surface to absorb the thermal energy. On account of this, the molten material cooled much faster than the amount of time required for it to settle. This was also stated by Gratzke *et. al.* [4] during conventional welding as solidification in the range of 10 to 100 ms tends to occur. In any case, the solidification of the laser beam would be in the same range or faster due to its high monochromaticity, coherence and uni-directionality which will cause similar effects to what Gratzke *et. al.* justified. However, further work in to accurate measurement of the cooling rate during HSLW of thin sheet steel is suggested herein which could justify this effect further.

5. Discussion

Up on considering the laser-material interaction found in this investigation and suggestions from previous research with regards to eliminating the hump, it can be further suggested that in order for the humping effect to be minimal and almost eliminated – it is necessary that the weld-bead length (in its cross-section) was broadened. From this work, it was found that the technique which produced the best result with smaller and relaxed hump gradients was firstly the PALW and then the Nd:YAG laser alone. This was because the Nd:YAG laser had a lower beam quality in comparison to that of the CO_2 laser which distributed a concentrated laser beam. In addition, the PALW produced the smoothest humps because of the additional heat source applied. This broadened the width and shortened the cross-sectional height of the laser welds. Having seen this, it can then be suggested that it is possible to minimize humping and even eliminate it by first applying a laser beam with slightly low quality (possibly a flat head, top-hat beam) which has a spread energy distribution with an additional heat source. In particular, the PALW technique acts as an elongated cooling tool for the weld whilst the laser beam already heats-up the material and causes it to melt. At the same time, the plasma torch elongates the rapid cooling effect and aids in distributing the weld more equally so that the humping gradient is much smaller. This concept goes well with previous researcher's statement of broadening the length-to-width ratio of the weld bead to eliminate the humping phenomenon [3, 4, 9, 10]. By observing the optical images of all the samples within this study, it can be denoted that humping occurs with most samples to various extent. However, undercut was not apparent. Drop out of the weld pool was evident during the CO_2 laser alone welding experiments, particularly, at low welding speeds, but was not consistent during the Nd:YAG laser alone and PALW experiments (see Figure 11 (a)). To investigate the occurrence of a ropey bead, a topographical analysis is required in future investigations which would confirm this effect. However, from analyzing the cross-section of various samples as previously shown in Figure 8, Figure 9 and Figure 11, it can be postulated that ropey bead would be formed throughout the weld seam.

To compare the mechanical strength of the welds, a tensile strength test was conducted. The RSWed samples comprised of an average ultimate tensile strength (UTS) of 998.84 MPa before it failed. This was the highest as one can see in Figure 12 from the set of welded samples that were tested. The average UTS measured for the PALW samples was 694.22 MPa, 565.20 MPa for the Nd:YAG laser alone and 492.42 MPa for the CO_2 laser alone sample.

For the MSWed sample, it was interesting to note that each sample fractured from either side of the weld bead rather than fracturing from the weld itself unlike the others. This proved that the MSW strength was much higher than that of the parent material itself, whereas for the other samples the fracture in turn occurred from the weld seam itself. Owing to the UTS value of the MSWed samples, it was indicative as to what mechanical strength the laser welded seam should comprise. However, all the laser welded samples were of much lower UTS than the RSW as seen from Figure 12. Having said that, the PALW samples were of higher mechanical strength than that of the Nd:YAG and the CO_2 lasers. Following was the Nd:YAG and then the CO_2 laser welded samples. This result correlated with the level of defects found in each of the samples and corresponded to the penetration depth. Since the PALWs comprised of the highest penetration and lowest level of welding defects than that of the Nd:YAG and the CO_2 laser, it was therefore clear that this sample comprised of a slightly better mechanical strength followed by the Nd:YAG laser and finally the CO_2 laser which comprised of much higher hump gradients. Owing to this, it was obvious that the quality of the laser welded samples in comparison to the conventional MSWed samples comprises of low mechanical strength within the laser welded seam. This was not sufficient enough to similarly match that of the RWS joint, since it had insufficient weld quality, as result of the humping onset. Therefore, it is suggested that future studies could entail a similar method for comparing the weld strength of relevant samples to the conventional welding process already in place.

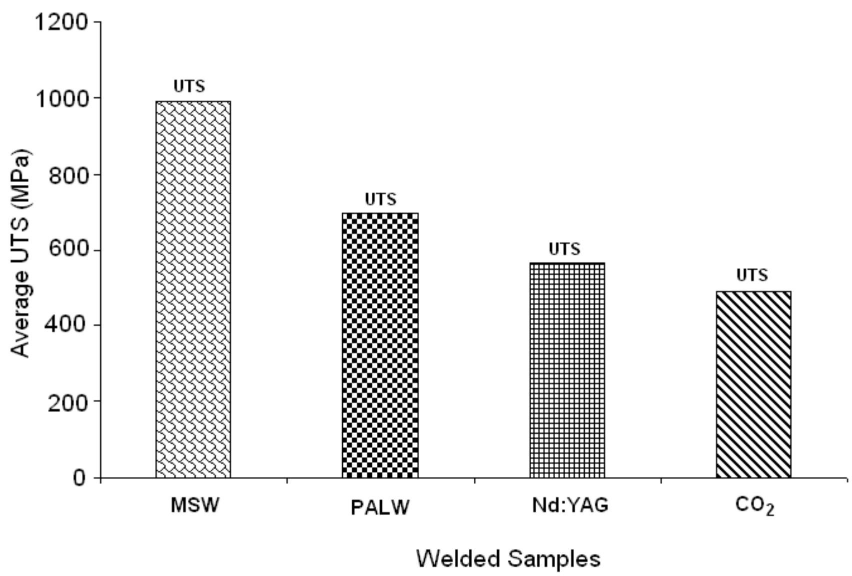

Figure 12 Average ultimate tensile strength of MSW, PALW and both the Nd:YAG and CO_2 laser alone welded samples of the FC.

For storage of food products, it is extremely undesirable if the weld seam of baked beans can or a tomato puree for example would consist of weld defects. This is because the FCs store sufficient amount of liquid which would be subject to leaking contamination, oxidation and exposure to corrosive metal. In addition, it is important that gases such as Ar and N_2 are used to preserve food inside the FCs, so that the laser weld is free from any defects to prevent the preservative gasses to escape. This will otherwise contaminate the food product considerably. Therefore, welding defects namely: brittle cracking in various forms; distortion; nuggets; porosity; lack of penetration and fusion; inclusions; humping; under-cut, and the occurrence of a ropey bead will reject the weld whilst the FC is passed through the pressure testing procedure. Thus, from a metallurgical aspect, the welded material must avoid the above defects and adhere to the appropriate mechanical strength and the quality standards set for canned food packaging products.

Furthermore, it is suggested that for future experiments should be carried using butt weld configuration. This will enable one to understand how the humping behavior may occur since humping has been observed during high speed welding only on bead-on-plate samples. In addition, a dimensional analysis of the weld-bead is also suggested which will further enable one to know the dimension of the welding discontinuities and in turn could assist by using a certain spot size of the laser as well as the intensity of the plasma torch to achieve the perfect height-to-length ratio in order to minimize and possibly eliminate humping. What is more, further work is also required on the suitability of the laser system by comparing with the current MSW machinery used for manufacturing the three-piece FCs. Further research is also suggested on the suitability of a correct motion system for the laser which comprises of a faster dynamic response. This will enable the welding process to achieve high speed since the work herein employed a rotary axis welding fixture which will not compliment a butt weld configuration when welding in a linier motion. Investigating the suitability of the a most appropriate motion system within a production set-up will require lengthy experimental studies once the laser welding process free from the aforementioned welding discontinuities is defined.

Moreover, a finite element model (FEM) using computational means could also be adopted to model the humping phenomenon at various speeds which will allow the prediction of the onset of the humps with respect to temperature and time at any traverse speed and other laser parameters employed. This will enable one to also understand the perfect energy density and the associated laser parameters as well as the most ideal traverse speed to be used for the HSLW of three-piece FC bodies.

6. Conclusion

This paper was focused on first a case study of a U.K. based FC manufacturer and its production system and the current process employed - rationalizing the implementation of the new HSLW process. Secondly, an experimental investigation was also conducted using a Nd:YAG, CO_2, and a PALW process complimented by a specially designed rotary axis welding fixture to further investigate the technical feasibility of the aforementioned process. The combined study revealed following conclusions:

- Upon the high demand for manufacturing three-piece FCs - mass production of the FC has become a necessity in order to meet the high production requirements.

- Employing the HSLW process could result in considerable savings on material utilization and lead-times. This in turn enables higher production capacity, production out-puts, reduce labour, maintenance cost and overheads leading to cost savings and profit for the packaging can manufacturers not only in Europe but also around the world.

- Experimental study showed that a regime of reduction in humping at increasing welding speeds resulted when all three laser techniques were applied. However, the CO_2 laser welded sample showed humping to be much steeper and narrow due to its high beam quality in comparison with the Nd:YAG laser alone and the PALWed samples.

- The Nd:YAG laser alone samples showed humping effect to be much relaxed in comparison to the CO_2 laser alone welded samples. The PALW technique showed a much relaxed hump and welding speed of up to 98 m/min showed some level of penetration within the tin-plated thin sheet steel.

- To avoid the humping effect, it is required that the melt-pool balances out evenly and a thicker weld bead is produced so that even spread of molten layer occurs. This is ideal with the aid of the PALW technique which offers an extra heat source.

7. Acknowledgement

This research received no specific grant from any funding agency in the public, commercial, or not-for-profit sectors. The author would like to thank Mr. Trevor Johnson and Dr Houzheng Wu for providing technical guidance and to all those associated with this research from the Advanced Joining Centre as previously known, at Coventry University (U.K.).

8. References

1. **Venkatesan, V.** Global demand for food containers to increase 3.8 % year through 2013, Asia food Journal, Bharat Book Bureau, **(Jan/Feb 2011 issue)**, P 08, www.asiafoodjournals.com.

2. **Livesey, F.** Value of food & drinks manufactured to the UK, *University of Cambridge Institute for Manufacturing Centre,* 2010, ISBN: 978-1-902546-86-5.

3. **Bradstreet., B. J,** Effect of surface tension and metal flow on weld bead formation, Welding Journal, 1968, **47**, 314 – 22s.

4. **Gratzke., U, Kapadia., P.D., Dowdent., J, Krooss., J,** and **Simons, G.** Theoretical approach to the humping phenomenon in the welding processes, 1992, **25**, 1640 – 1647.

5. **Mombo-Caristan., J. C, Mueller., R. E, Sharp., C. M., and McCay., M. H.** Parabolic Mirror Adapted- Alignment for High Speed-High Power Laser Welding with an oblong focused beam spot, Proceedings of the international Congress on application of lasers & electro-optics 1997, Section G, 191 – 199.

6. **Braunsteiner., A, Bhrer., M,** and **Schuocker., D,** High speed thin metal sheets welding with high power CO_2 lasers, *Society of optical engineering*, 1998, **3268**, 57 - 61.

7. **Cao, X,** and **Jahazi, M,** Effect of welding speed on butt joint quality of Ti–6Al–4V alloy welded using a high-power Nd:YAG laser, *Optics and Lasers in Engineering*, 2009, **47**, 1231 – 1241.

8. **A.S.H. Kabir, X. Cao, M. Medraj, P. Wanjara, J. Cuddy and A. Birur**, Effect of Welding Speed and Defocusing Distance on the Quality of Laser Welded Ti-6Al-4V, Material Science and Technology (MS&T), 2010, 2787 – 2797.

9. **Blundell., N, Biffin., J, Johnson., T.A., and Page, C.** High Speed Augmented - Laser welding of thin sheet metals, 5th internal conference on trends in welding research, Pine Mountain, Georgia, 483- 487.

10. **Page., C, Devermann., T, Biffin., J,** and **Blundell, N.** Plasma Augmented Welding and it's Applications. *Science and Technology of Welding and Joining*, 2002, **7**, No. 1.

11. **Russ, A., Leimer, M.,** and **Dausinger, F.** High Speed Micro Welding of thin Metal Sheets, Fifth International Conference on Laser Precision Micro Fabrication, Proceedings of SPIE 2004, **5662**, 300 – 305.

12. **Soderstrom., E., and Mendez., P.** Humping mechanisms present in high speed welding, Science and Technology of Welding and joining, 2006, **11 (5)**, 572 – 579.

13. **Romanko., A, Berry., D,** and **Fox., D,** Simulation of double seaming in two-piece aluminium can, Materials Processing and design: Modeling, Simulation and Applications, NUMIFORM, 2004, 1526 – 1532.

14. **Perry Equipment Corporation** (ISO9001), *Three-Piece Can Manufacturing,* Application data sheet 2007, EL-GI-AD-07.

15. **Steen, W.** and **Mazumder, J.** *Laser Material Processing, 4th Edition*, 2010, (Springer-Verlag London).

16. **Huang., Q, Hagstrom., J, Skoog, H.,** and **Kullber, G.** Effect of CO_2 laser parameter variation on sheet metal welding. *International Journal for the joining of materials*, 1991, **3**, 79 - 87.

17. **Seto, N., Katayama, S.,** and **Matsunawa, A.** High Speed Simultaneous observation of plasma and keyhole behavior during high power CO_2 laser welding: effect of shielding gas on porosity formation. *Journal of Laser Applications*, 2000, **12**, 245 – 250.

18. **Abe, N., Kunugita, Y.,** and **Miyake, S.** The Mechanism of High Speed Leading Path Laser Arc-combination Welding. Proceedings of ICALEO 98 (Orlando, U.S.A.) LIA 1998, **85** Section F, 37 – 45.